

# Low Reynolds Numbers LDA-Experimental Analysis of the Near-Field of an Isothermal Laminar Round Free Jet

A. Abbassi<sup>1,2</sup>, N. Kechiche<sup>1</sup>, and H. Ben Aissia<sup>1</sup>

**Abstract:** Jet transition towards a turbulent state is an interesting topic requiring a detailed analysis of the process leading to the onset and amplification of small flow disturbances. Here we examine experimentally the transition process for an isothermal laminar round free jet at low values of the Reynolds number. Close to the inlet nozzle, the turbulence intensity is assumed to be small enough so that the initial shear layer can be considered laminar and the velocity profile uniform. Experimental data are obtained using a Laser Doppler Anemometry (LDA) technique at various longitudinal and transversal coordinates,  $(x, y)$ . Spectral analysis of the instantaneous streamwise velocity component  $u(y, t)$ , at fixed stations  $x$  measured from the nozzle exit, reveals that the entrainment physical mechanism, which occurs by engulfment, is caused by the presence of coherent structures. However, in proximity to the jet center, the energy spectrum of the  $u(x, y = 0, t)$  velocity component proves the existence of a preferred mode (most unstable mode) of instability that has a convective nature. Our results compare well with those obtained using another experimental method based on laser tomography.

**Keywords:** Round jet, coherent structures, transition, LDA, Fourier transform, entrainment, preferred mode, velocity profile.

## 1 Introduction

The study of transition process from a laminar state to a turbulent one in shear flow, which is interesting for many potential industrial applications, dates from the early 1970's as explained by the fundamental paper of Crow and Champagne [Crow and Champagne (1971)]. It has since been found that this behavior is caused by the development, evolution and interaction of coherent structures mechanism [Winant and Browand (1974); Ho and Huang (1982)]. A possible scenario which may explain the mechanism of interaction of the coherent structures is made by Ho [Ho

---

<sup>1</sup> Unit of Metrology and Energetic systems, UR11ES59, ENIM, Tunisia

<sup>2</sup> Corresponding Author: Email: ali\_persomail@yahoo.fr

(1981)]. In fact, he interpreted the relationship between sub-harmonic instability and the vortex merging occurrences, responsible of the flow spreading and momentum transfer, by a sub-harmonic evolution model. This model explains the mechanism of vortex merging by the primary instability amplification added to the mean flow, which is the catalyst of the transition process. Thus, understanding the transition phenomenon and underlying physical mechanisms, which passes through the study of development of primary instability, is appreciably interesting. Indeed, for engineering purposes, such as the design of the burners of the combustion chamber, where it is desirable having a high-level of mixing and heat transfer, it is useful that the flow must be turbulent. Accordingly, it is worth knowing how to control the flow. In fact, the issue of flow control has attracted a great deal of attention over the last years due to the wide range of its potential industrial applications, like for instance, noise suppression due to vortex pairing [Gutmark and Grinstein (1999)].

Shear flows, such as jets, mixing layers, and wakes are present in many industrial flows which have different configurations of mixers and injectors. Free round jet, which is the object of the present paper, is obtained when a certain amount of momentum is fed from a circular nozzle into an unconfined environment at rest filled with the same fluid [Danaila (1997)]. Then the source of momentum spreads into the space, when advancing in the streamwise direction, free from the influence of external forces. In the region very close to the inlet nozzle the resulting free shear layer is round. An interesting physical mechanism, which is the source of the spreading process, occurring in the jet flow is the entrainment of external fluid from the irrotational flow region into the core of the shear layer [for more details, see for example Ben Aissia (2002)a; Abbassi, Kechiche, and Aissia (2007); Abbassi and Aissia (2014) ]. It is found that the entrainment process occurs by two different mechanisms: viscous diffusion and engulfment. The last mechanism is caused by the presence of coherent structures due to the development and amplification of the initial instability. This initial instability, caused by the velocity difference across a thin shear layer which is a necessary condition for instability [Rayleigh (1880)], is the so-called Kelvin-Helmholtz instability. It is worth to note that, the initial instability can be treated, in a satisfactory way (small disturbances approximation that is valid in the initial shear layer), by the linear stability theory which provides that two modes of instabilities occur in free round jets: varicose mode and sinuous mode [Danaila (1997)]. In addition, it is found that, except at very low Reynolds numbers, the laminar thin shear layer with constant density ( $\rho_j/\rho_\infty = 1$ ) is unstable to any small disturbances added to the flow. Furthermore, Hussain and Zaman show that these disturbances advance by selective amplification as they convect in the streamwise direction of the flow [Hussain and Zaman (1985)]. Then the formation of the axisymmetric or helical structures, as a result of the vorticity mi-

gration, caused by the instability is accompanied by large amplitude fluctuations. Noting that, through linear and non-linear interactions, coherent structures formation and merging processes occur downstream of the shear layer and significantly contributes to the entrainment, mixing of the physical process by convective transport (marked by the jet transverse spreading) [Winant and Browand (1974)], and acoustic noise generation [Kibens (1980); Crighton (1975)].

The present work sheds light on the physical mechanisms behind the development of the unstable modes encountered in the transition region of sheared flows. This issue is analysed experimentally by studying the near-field of a free round, downward and isothermal jet ( $T_0/T_\infty = 1$ ) with an initial uniform velocity profile [Abbassi and Aissia (2014)]. We have chosen conditions for which the flow is incompressible and free from the influence of the buoyancy forces with a long laminar zone as suggested by Ben Aissia [Ben Aissia (2002)]. The local measurements are performed using Laser Doppler Anemometry (LDA) experimental technique. It is noticed that the region of interest, where the Kelvin-Helmholtz instabilities develop, is limited to the zone close to the nozzle exit. A local instantaneous data of the longitudinal velocity component  $u$  is obtained along both  $x$  and  $y$  directions, i.e.  $u(x, y, t)$ . Through statistical analysis, using the streamwise velocity  $u$  data, the initial shear layer close to the inlet nozzle is first examined. The fundamental instability frequency and entrainment phenomenon are obtained by studying the energy spectra of the streamwise velocity via of Fourier transform. Therefore, the results suggest that the most unstable mode in the primary transition region at Reynolds number is equal to 830, for the free round jet, is the sinuous mode (helical mode).

## 2 Experimental apparatus and procedure

The experimental setup employed in the present paper was used in our previous work and will be summarized herein [Kechiche, Abbassi, Filali, Jay, and Aissia (2009)]. Indeed, experiments were carried out on an isothermal free round laminar jet of fluid air. The flow is generated by a circular nozzle of internal diameter equal to  $d_{jet} = 12.4\text{mm}$  and spreads freely into an unconfined air medium. The emission velocity profile  $\bar{u}_{jet}$  has a uniform shape and measurements were performed by means of Laser Doppler Anemometry (LDA) in forward scatter mounting Fig. 1 (for more details see [Ben Aissia (2002)]). The measurement chain contains mainly: a filter with low porosity ( $0.8\mu\text{m}$ ), used to remove the impurities, such as the water droplets, which are responsible for the distortion of the LDA measurements, a valve punch placed downstream allows a manual regulation of the outflow rate; consequently the Reynolds number  $Re = \bar{u}_{jet}d_{jet}/\nu$ , (where  $\bar{u}_{jet}$  is the mean velocity,  $d_{jet}$  is the internal diameter of the nozzle and  $\nu$  is the kinematic viscosity of air), at the inlet nozzle is well-defined. In order to make measurements

with LDA method feasible, air is mixed with incense particles with a diameter varying between 0.5 and 5 $\mu\text{m}$  and with a well-studied concentration. Then, air flow is passed through a laminariser composed by a honeycomb and screens to obtain a laminar flow at the nozzle exit [for more details see, Ben Aissia (2002), Zaouali (2004)].

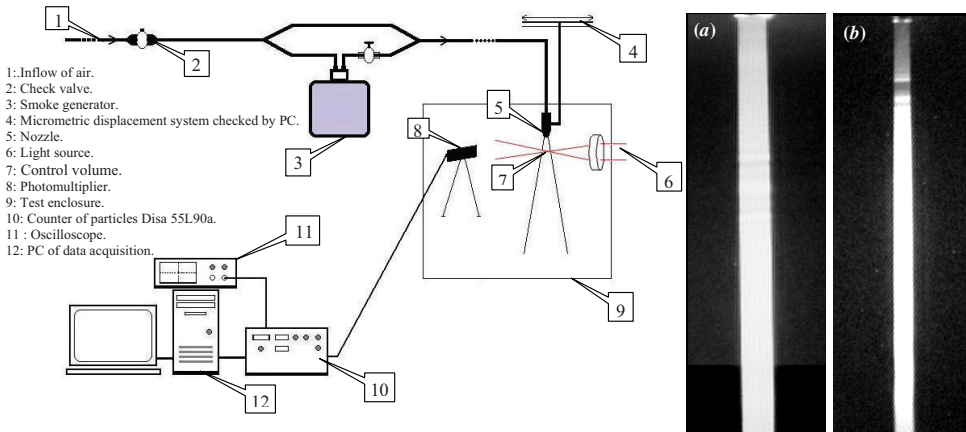


Figure 1: Schematic of the measurement region definition, instrumentation [Kechiche, Abbassi, Filali, Jay, and Aissia (2009)] and the characteristics of the jet initial shear layer obtained by the laser tomography technique. (a) Laminar length  $x/d_{jet} = 17.5$  for  $Re = 832$ . (b) Laminar length  $x/d_{jet} = 34$  for  $Re = 586$ .

The optics and acquisition chain are described in details in [Ben Aissia (2002); Zaouali (2004)]; Kechiche, Abbassi, Filali, Jay, and Aissia (2009)]. The jet expands freely into an unconfined medium; consequently it is very sensitive to the external perturbances. To isolate the flow from external disturbances, the entire system is enclosed in a 6m<sup>3</sup> noise reduction Plexiglas chamber as shown in Fig. 1. In the present study the data, which only concerns the axial velocity component  $u$ , were obtained by Laser Doppler Anemometry (LDA) for various  $xy$  stations. The signals are digitized at a sampling rate of 100kHz and will enable us to observe the principal frequencies of the coherent structures at various  $xy$ -coordinates of the jet flow. In each measurement, 4096 samples were acquired corresponding to a signal duration of 40ms. A non uniform step in the  $x$ -direction is used. At the inlet nozzle the step used is equal to 10mm, after the potential core we have increased the step to reach 20mm to be able to go farther downstream in the flow direction. The Fourier analysis has been widely used to characterize flows in which interacting modes are dominant [Yilmatz and Kodan (2000)] and will be used in the present investigation.

### 3 Results and interpretations

The analysis of results issued from the experimental measurements of an isothermal laminar free round jet covers the entire near-field region. In the present study, the parameters used include the Reynolds number  $Re$ , and the Strouhal number  $Str$  which are defined, respectively by  $Re = \bar{u}_{jet}d_{jet}/\nu$  and  $Str = fd_{jet}/\bar{u}_{jet}$ , where the  $\bar{u}_{jet}$  represents the mean velocity measured at the inlet nozzle,  $d_{jet} = 12.4\text{mm}$  defines the internal diameter of the nozzle,  $\nu$  is the air viscosity, and  $f$  represents the frequency of the instability harmonic. The previous choice, of control parameters, will allow us to situate ourselves compared to other works. In addition to the hypothesis taken into account in paragraph §2, we have assumed that, the gravity effects due to the density differences between the ambient air and that forming the jet mixed with incense is negligible, i.e. the Froude number  $Fr$  is taken very large. The operating Reynolds numbers throughout the experiment was taken sufficiently high, remaining in the limit of small Mach number ( $M_0 \ll 1$ ), which allows the laminar flow to be justified Fig. 1a and Fig. 1b (tomography images). Also, the pressure is hydrostatically distributed throughout the jet flow.

#### 3.1 The inlet flow conditions

In this section, the initial boundary layer at the inlet jet is first studied to ensure that it is laminar.

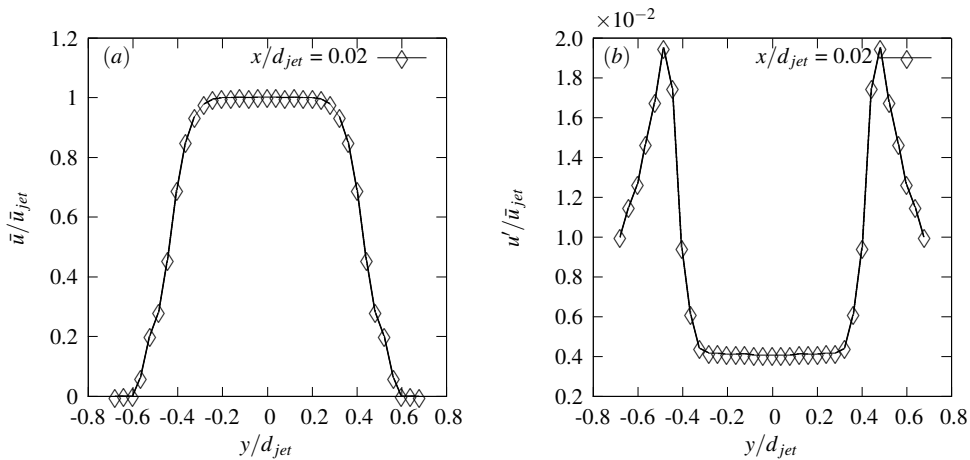


Figure 2: Characteristics of the initial shear layer of the jet measured at the inlet nozzle. (a) Transversal evolution of the mean streamwise velocity  $\bar{u}/\bar{u}_{jet}$ . (b) Transversal evolution of the turbulence intensity  $u'/\bar{u}_{jet}$ .

In fact, the analysis in this section concerns the natural development and amplification of the hydrodynamic instabilities. Consequently, the measurement of the turbulence intensity very close to the outlet of the nozzle is made. This quantity, evaluated through  $u'/\bar{u}_{jet}$ , is defined as the root-mean-square of the turbulent velocity normalized by the initial mean jet velocity  $\bar{u}_{jet}$  and is given by the following equation

$$\frac{u'}{\bar{u}_{jet}} = \sqrt{\langle (u - \langle u \rangle)^2 \rangle} / \bar{u}_{jet} \quad (1)$$

where  $\langle u \rangle$  denotes the temporal averaged value of the velocity  $u(t)$ . In Fig. 2a, we are representing the transversal evolution of the jet mean velocity  $\bar{u}_{jet}$  very close to the inlet nozzle, at the section of coordinate  $x/d_{jet} = 0.16$  which is selected as close as possible to the nozzle outlet making feasible the LDA measurements. Noting that, the momentum thickness  $\theta_0$  based on the initial mean velocity is about 5mm, which corresponds to a laminar mixing layer at the exit region [Abid and Brachet (1993)]. The transversal evolution (as a function of the radial coordinate,  $y/d_{jet}$ ) of the turbulence intensity, very close to the inlet nozzle ( $x/d_{jet} = 0.16$ ), is given by Fig. 2b. It is worth to note that, the level of the turbulence intensity at the jet center is low and remains less than 0.4% for an initial velocity value equal to  $\bar{u}_{jet} = 1.04\text{m/s}$ , which corresponds to a Reynolds number equal to 830. However, at the jet boundaries the magnitude of this quantity increases. This behavior can be, perhaps, explained by the vortex development in the mixing region of the jet flow with the surrounding environment. In addition, noting that the value of this quantity is in the same range as that found in the experimental study released by Reynal [Reynal, Harion, Favre-Marinet, and Binder (1996)]. Indeed, these authors present in their study an averaged rate of turbulence about 0.5% up to 1.5% at the centerline jet and for a comparable range of Reynolds numbers. This result represents a first validation of the measurement method used herein and in our previous work [Kechiche, Abbassi, Filali, Jay, and Aissia (2009)]. However, it is worth to note that the low-level of turbulence intensity obtained herein can be reduced furthermore by improving the structure of the nozzle. Indeed, in their study Yu [Yu and Monkewitz (1993)] obtained a turbulence intensity level, in the region of the initial shear layer, less than 0.06%.

### 3.2 The mean flow fields

Statistical moments, such as the mean and the variance of the streamwise velocity component, are obtained by analysing a set of  $u^{(k)}(\mathbf{x})$ ,  $k = 1 \dots N$  data that contain  $N$  statistics samples measured at the point of position  $\mathbf{x}$ , where  $\mathbf{x}$  is the coordinate

vector. Indeed, the average velocity value is typically calculated by the following equation:

$$\langle u(\mathbf{x}) \rangle = \frac{1}{N} \sum_{k=1}^N u^{(k)}(\mathbf{x}) \tag{2}$$

and for each random process realization  $u^{(k)}(\mathbf{x})$ ,  $k = 1 \dots N$ , the velocity fluctuation is defined by the following relation:

$$u'^{(k)}(\mathbf{x}) = u^{(k)}(\mathbf{x}) - \langle u^{(k)}(\mathbf{x}) \rangle \tag{3}$$

To calculate the variance of the streamwise velocity  $u$  we used the following formula:

$$\sigma_u^2 = \langle u'^2(\mathbf{x}) \rangle = \frac{1}{N} \sum_{k=1}^N \left\{ u'^{(k)}(\mathbf{x}) \right\}^2 \tag{4}$$

Noting that, the study of the unsteady turbulent flow requires quantities that can precisely characterize the turbulence such as the mean field and the standard deviation of the velocity fluctuations, but also by the parameters of spatial length and/or time scales.

The first results, that will be presented in the next sections, concern the shape of the streamwise velocity profiles at several longitudinal stations located at the  $x/d_{jet}$  coördinate. In fact, this information is significantly interesting since a necessary condition of flow instability is met when the basic velocity profile has an inflection point [Drazin and Reid (1981)]. Also, this quantity will allow us to calculate the different variables of the jet such as  $\theta$  and  $R_u/\theta_u$ . Indeed, the momentum thickness, which is defined by  $\theta = \int_{\mathbb{R}^+} \frac{u}{\bar{u}_{jet}} \left( 1 - \frac{u}{\bar{u}_{jet}} \right) dy$ , has a value equal to,  $\theta_0 = 5\text{mm}$  at the inlet nozzle, i.e. at the  $x$ -coördinate equal to  $x/d_{jet} = 0.1613$ , obtained for the initial velocity equal to  $\bar{u}_{jet} = 1.04\text{m/s}$ , i.e. for a Reynolds number  $Re = 832$ . In brief, the standing of the present study comes from the fact that the jet develops freely at low Reynolds number; consequently it is very sensitive to small external perturbations, and there are few studies on that range.

### 3.2.1 Evolution of the $R_u/\theta_u$ quantity

The figure Fig. 3 shows the evolution according to the streamwise coördinate  $x/d_{jet}$  of the interesting parameter  $R_u/\theta_u$ , where  $R_u$  is the inlet radius, for measurement data released in the present work and compared with the empirical formula given by Crighton and Gaster [Crighton and Gaster (1976)] and that obtained by Plaschko, [Plaschko (1979)] (which is given by the formula  $R_u/\theta_u = (0.06(x/d_{jet}) + 0.04)^{-1}$ ).

We remark that the figure shows a qualitative agreement (the decreases according to the  $x/d_{jet}$  coordinate) between the different formulas describing the evolution of this parameter. Noting that, the difference between these results is related to the experimental conditions of each author. This result provides a validation for both measurements performed in the present study and the calculation method used.

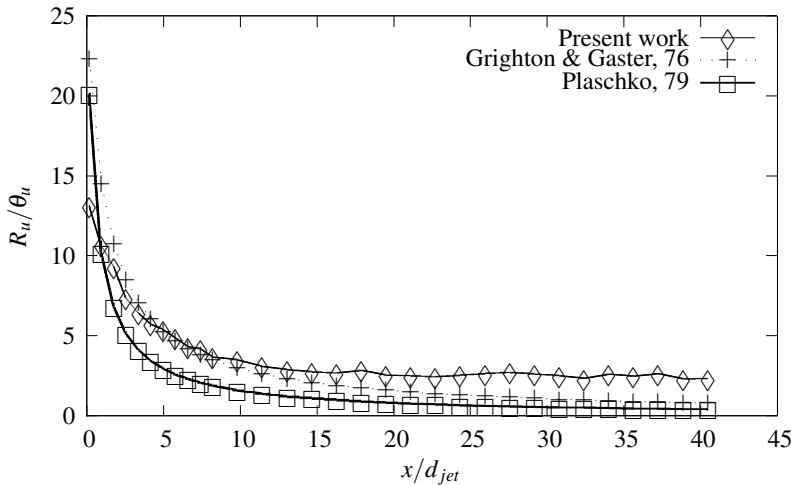


Figure 3: Statistical results for the jet ( $Re = 832$ ). Evolution of the  $R_u/\theta_u$  ratio along the streamwise direction and compared with the empirical formulas given by Grighton and Gaster [Grighton and Gaster (1976)] and Plaschko [Plaschko (1979)].

It is worth to note that, the  $R_u/\theta_u$  parameter is a data obtained from experience, which is the only link to adjust the mean velocity as a function of the streamwise coordinate for an analytical study of the flow. Indeed, this parameter determines the nature of the most unstable mode which develop in the jet. Thus, for small values of this parameter, i.e. for locations downstream from the inlet nozzle, only the helical mode is the most unstable mode [Batchelor and Gill (1962)]. Contrariwise, for large values of  $R_u/\theta_u$ , the jet behaves identically to a plane mixing layer and the most unstable mode is axisymmetric with the coexistence of other non-axisymmetric modes.

### 3.2.2 Evolution of the mean velocity

In this paragraph, we are going to present the dynamic property of the flow as given in figures Fig. 4 and Fig. 5. In figure Fig. 4, we represent the evolution of the mean streamwise velocity  $\bar{u}/\bar{u}_{jet}$ , while in the Fig. 5 we show the  $\bar{u}/\bar{u}_c$  variation, for sev-

eral streamwise coordinate  $x/d_{jet}$ . These figures show that, the evolution of the mean velocity  $\bar{u}$  has a constant value for the low values of the longitudinal position  $x/d_{jet}$  which proves the classical result of the existence of a potential core region as demonstrated in several previous studies for example [Abbassi and Aissia (2014); Ben Aissia (2002)]. This result is also a validation of the calculation procedure and the measurements undertaken by the LDA technique. Noting that, for the large

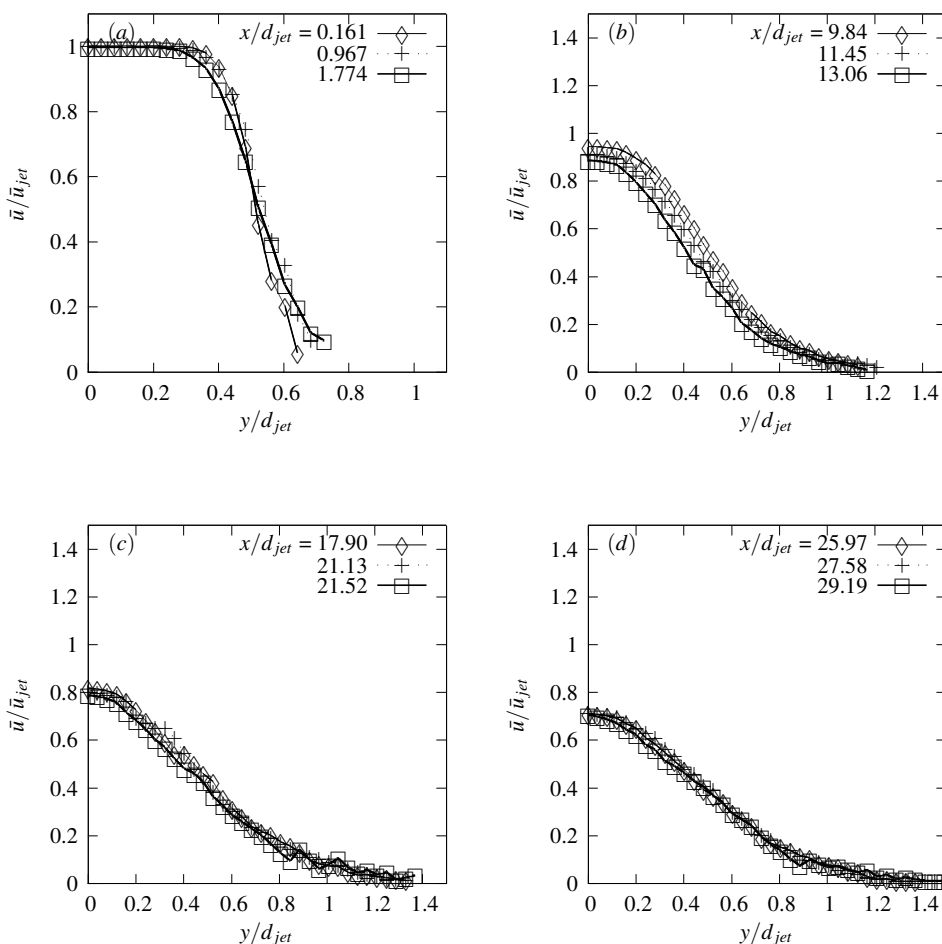


Figure 4: Evolution of the axial mean velocity  $\bar{u}/\bar{u}_{jet}$  for various streamwise locations defined by the  $x/d_{jet}$  coordinate.

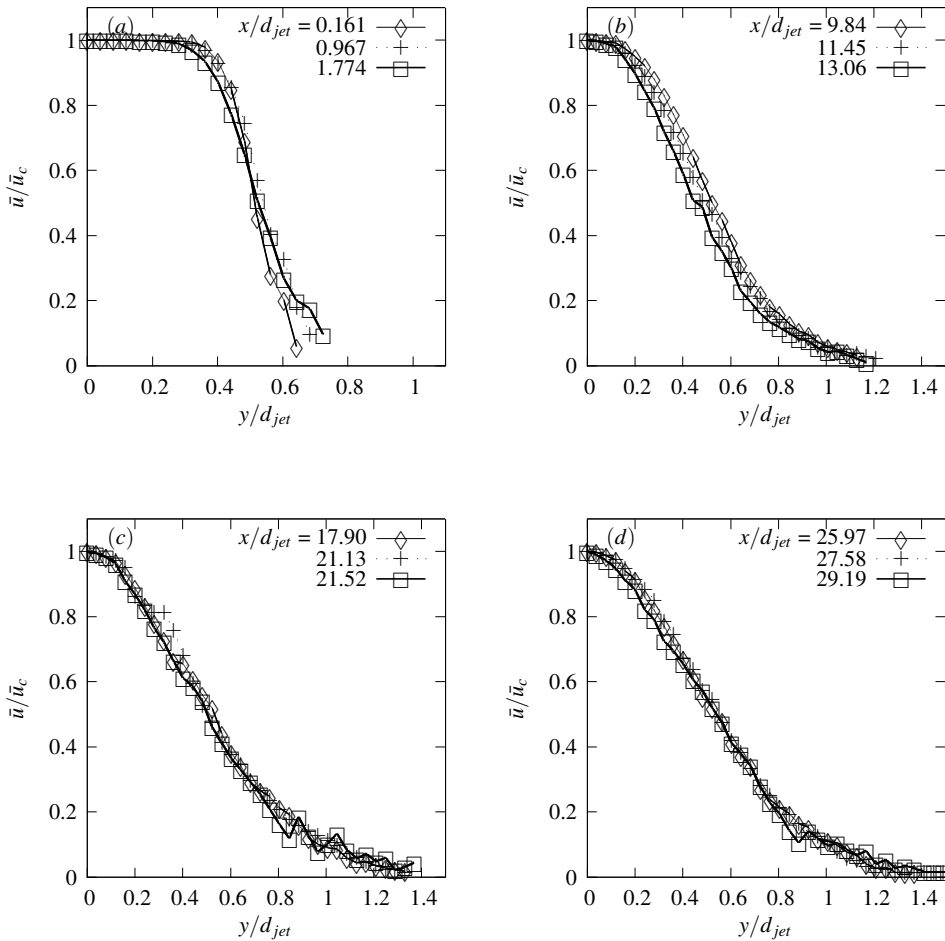


Figure 5: Evolution of the axial mean velocity  $\bar{u}/\bar{u}_c$  for various streamwise locations defined by the  $x/d_{jet}$  coordinate.

streamwise distances  $x/d_{jet}$  the potential core region disappears due to the entrainment of the ambient air into the jet flow. As a result of the entrainment process, the centerline jet velocity is decreased as shown in Fig. 6.

In addition, figure Fig. 6 shows the evolution of the jet thickness,  $\theta$ , as a function of the streamwise locations  $x/d_{jet}$ . It is worth to note that, as we are advancing farther downstream in the flow direction; the jet undergoes a section enlargement caused

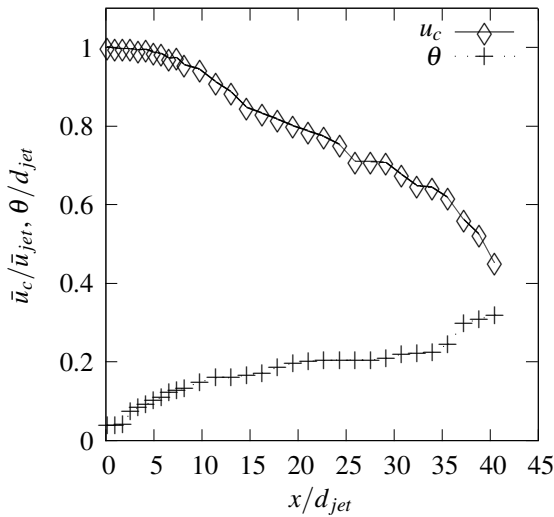


Figure 6: Evolution of the streamwise mean centerline jet velocity  $\bar{u}_c/\bar{u}_{jet}$  for  $y/d_{jet} = 0$  and evolution of the jet thickness  $\theta$ .

by the increasing amount of the surrounding air added to the flow and marked by the decrease of the centerline velocity. These results are in good agreement with results obtained numerically in previous papers [see Ben Aissia (2002); Ben Aissia (2002); Abbassi and Aissia (2014) for a detailed description].

### 3.3 Unstable mode of the jet: preferred mode

To make the streamwise velocity signals  $u$ , obtained from LDA measurements usable, a pre-analysis phase should be performed. Indeed, this operation determines the basic properties of the original signals such as frequency, structure of background noise, signal to noise ratio, non-stationarity, etc. In the present paragraph we are going to present the conventional spectral analysis method based on Fourier transform, which is an interesting tool in signal analysis, applied to the LDA velocity time series. Indeed, a frequency description is more often "readable" compared to the temporal description. The Fourier transform associated with a continuous time signal  $u(t)$  is obtained by  $TU(f) = \int_{-\infty}^{\infty} u(t) e^{-j2\pi ft} dt$ , which decomposes, in a canonical way, the signal in linear combinations of elementary waves. However, the LDA streamwise velocity time series ( $u$ ) are sampled signals, i.e. discrete time signals. Thus, sampling the continuous signal  $u(t)$  with a sampling period

$T_e (F_e = 1/T_e)$  gives a discrete signal  $u[n] = u(NT_e)$  whose Fourier transform is  $1/T_e$ -periodic. In order to avoid any recovery problems and to be able to reconstruct the original signal, it is necessary that the Shannon condition is met:  $T_e < (1/2)B$  with  $B$  is the bandwidth of the signal. Under the previous conditions, the discrete Fourier transform is then expressed as follows:

$$TU(f) = T_e \sum_{n \in \mathbb{Z}} u[n] e^{-j2\pi n f T_e} \quad (5)$$

### 3.3.1 In the near-field jet

Unlike to the helium jet, the instability in the flow of a homogeneous air jet doesn't have a global character. To demonstrate this behavior, we proceed to a Fourier analysis of the velocity time series measured by Laser Doppler Anemometry LDA. Noting that, data acquisition of measurement points doesn't occur at regular time intervals and then should be resampled in order to use the Fast Fourier Transform FFT algorithm. Accordingly, we choose an "acquisition frequency" equal to twice the average LDA acquisition frequency. In the next paragraph, the study of the local streamwise velocity signal  $u(x, y, t)$ , is first performed for two longitudinal stations defined by the  $x/d_{jet}$  coordinate and for two transversal positions defined by the  $y/d_{jet}$  coordinate. Noting that, the first point is taken close to the inlet nozzle while the other point is given at the position away from of the potential core.

The times series and energy spectra of the streamwise velocity component  $u$ , issued from the LDA measurements, are given in figures Fig. 7 and Fig. 8. Fig. 7, shows the spectra close to the inlet nozzle and in the shear layer region, located at  $x/d_{jet} = 0.16$  and  $y/d_{jet} = 0.48$  while the Fig. 8 gives the spectra at the centerline jet far the potential zone. Noting that, in the vicinity of the inlet nozzle Fig. 7b, corresponding to the streamwise position  $x/d_{jet} = 0.16$  and in the shear layer region, the energy spectra of the velocity presents a frequency peak of value approximately equal to  $f\theta/\bar{u}_{jet} = 0.015$ , where  $f$  represents the frequency and  $\theta$  is the local jet thickness. We remark that, the obtained value is a characteristic of the *shear mode* and is in good agreement with the typical experimental values found in the literature for this kind of instability ( $0.01 < f\theta/\bar{u}_{jet} < 0.023$ ) [Gutmark and Ho (1983)]. However, the jet preferred mode is often observed in the zone farther downstream of the potential core region. In Fig. 8b, the dominant frequency is detected in the energy spectra of the velocity at the longitudinal position equal to  $x/d_{jet} = 9.84$ . It is worth to note that, the obtained value of the dominant frequency gives a value equal to  $f\theta/\bar{u}_{jet} = 0.25$  for the Strouhal number; which is a characteristic of the preferred jet mode experimentally observed. We remark that the value of the Strouhal number is in the range of values found in the literature ( $0.24 < fd_{jet}/\bar{u}_{jet} < 0.5$ ). This result

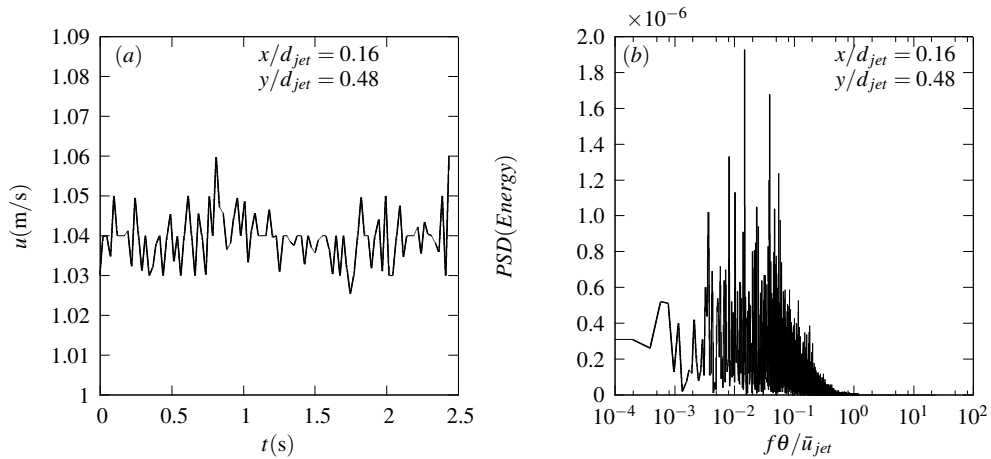


Figure 7: Temporal spectra of the streamwise velocity at the region close to the inlet nozzle of the air round jet (emission velocity equal to  $\bar{u}_{jet} = 1.04m/s$  corresponds to a Reynolds number equal to  $Re = 832$ ). (a) Time series of the streamwise velocity  $u$  at the edge of the inlet nozzle. (b) Spectra of energy, obtained by the Fourier transform, at the nozzle inlet.

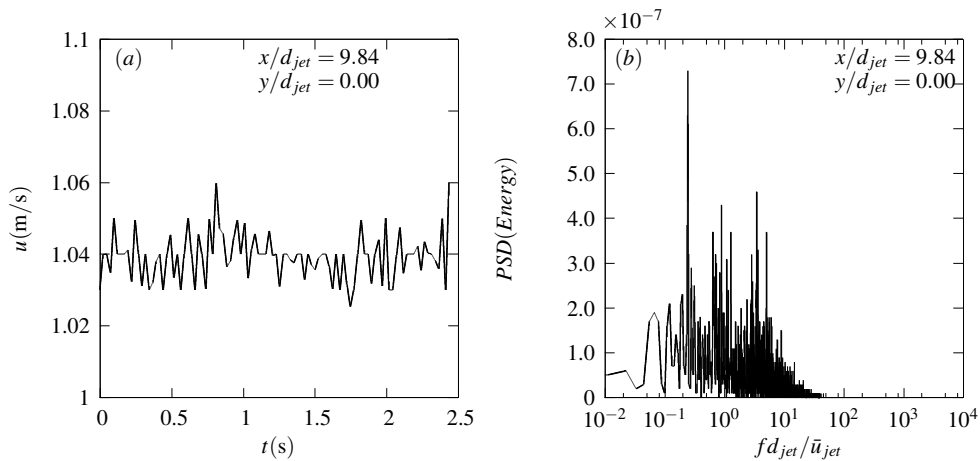


Figure 8: Temporal spectra of the streamwise velocity at the region far from the potential core of the air round jet (emission velocity equal to  $\bar{u}_{jet} = 1.04m/s$  corresponds to a Reynolds number equal to  $Re = 832$ ). (a) Time series of the streamwise velocity  $u$  at the jet centerline. (b) Spectra of energy, obtained by the Fourier transform, downstream the potential core region.

constitutes a validation of the procedure used and the measurements made by LDA in the present work. Based on the results previously obtained and unlike wakes or mixing layers flows, jet flow has two different scales for instability: *i*) firstly, in the region close to the jet exit the scale which governs the nature of the instability frequency of the shear layer is the jet thickness defined by  $\theta$ , and *ii*) secondly, in the zone farther downstream of the potential core region it is the internal nozzle diameter defined by  $d_{jet}$  which dictates the frequency of the preferred flow mode.

### 3.3.2 In the jet shear layer region

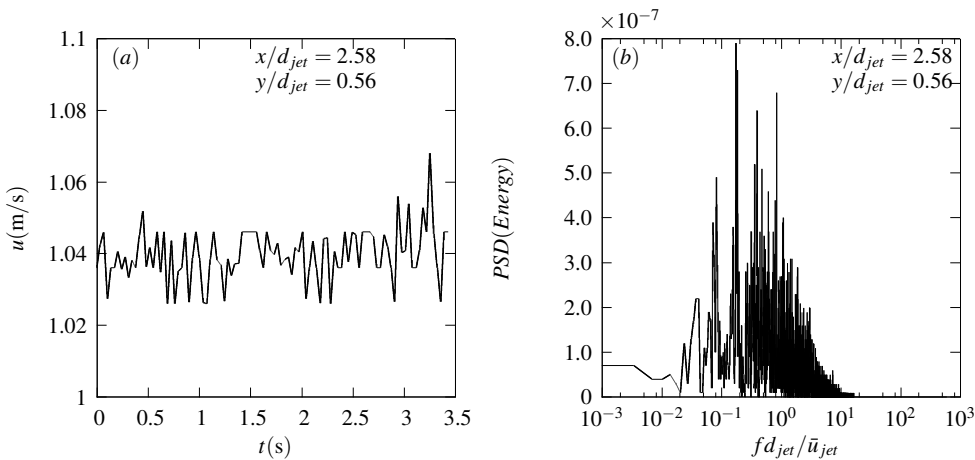


Figure 9: Temporal spectra of the streamwise velocity at the shear layer region of the air round jet (emission velocity equal to  $\bar{u}_{jet} = 1.04m/s$  corresponds to a Reynolds number equal to  $Re = 832$ ). (a) Time series of the streamwise velocity  $u$  at the shear layer region. (b) Spectra of energy, obtained by the Fourier transform, at several downstream positions.

In the present paragraph, we are going to present the study of the most unstable mode evolution as shown in figures Fig. 9 and Fig. 10. In fact, in these figures we are interested in the spectral analysis of the longitudinal velocity component  $u$  in the shear layer region of the jet flow defined by the transversal coordinate equal to  $y/d_{jet} \sim 0.56$  and for longitudinal distances  $x/d_{jet}$  ranging up after the end of the potential core. It is remarkable to note that the evolution of the sub-harmonic mode defined by the quantity  $fd_{jet}/\bar{u}_{jet} \approx 0.187$  is obvious from these figures. Noting that for the streamwise station defined by the longitudinal coordinate equal to

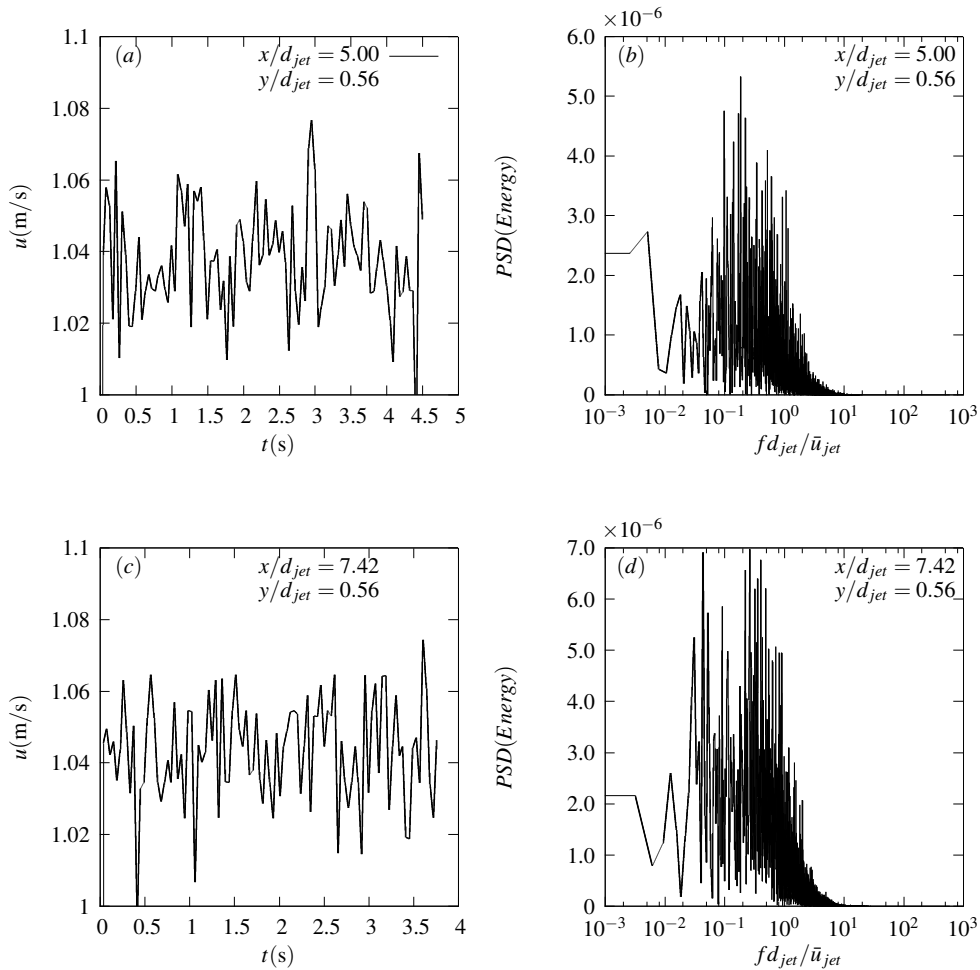


Figure 10: Temporal spectra of the streamwise velocity at the shear layer region of the air round jet (emission velocity equal to  $\bar{u}_{jet} = 1.04m/s$  corresponds to a Reynolds number equal to  $Re = 832$ ). (a – c) Time series of the streamwise velocity  $u$  at the shear layer region. (b – d) Spectra of energy, obtained by the Fourier transform, at several downstream positions.

$x/d_{jet} = 2.58$  the most unstable mode is the preferred mode, even with the existence of others sub-harmonics which appear in the spectra Fig. 9b. As we are going farther downstream in the flow direction and for the streamwise station defined by the longitudinal coordinate equal to  $x/d_{jet} = 5.0$  which is the region after the po-

tential core, the preferred mode of the jet persists as the most unstable one as shown in the Fig. 10b. Indeed, the most energetic peak frequency defines a characteristic of this type of instability mode. Note that, for the streamwise position given by the coordinate value equal to  $x/d_{jet} = 7.48$  the jet preferred mode doesn't exist and the other sub-harmonics modes become increasingly significant as shown by Fig. 10d. It is significant to note that, on the one hand, the last energy spectra located at the longitudinal coordinate  $x/d_{jet} \approx 8$ . the coexistence of diverse energy modes almost in the same magnitude, when the jet flow reaches an advanced state in the process of the turbulence transition, makes the identification of the unstable modes very fastidious. On the other hand, we can still discern a significant peak frequency around the sub-harmonic mode as shown in the Fig. 10b. It is worth to note that this behavior, namely the existence of a natural sub-harmonic mode in the last energy spectra Fig. 10b, can be explained by an alternating arrangement and merging phenomenon of the coherent structures which develop in the jet shear layer region. Noting that from the inlet nozzle zone until the end of the potential core region, the primary rings move downstream at the convective velocity  $u_c$  and with a separation distance between structures equal to  $L$ , resulting in a preferred mode frequency given by the quantity  $f_p$  evaluated by the formula  $f_p = U_c/L$ . It is significant to remark that once the pairing is achieved by alternating, with the hypothesis that the convection velocity is the same for all coherent structures, the distance between two vertices in the shear layer jet region, which is characterized by a high velocity gradients, becomes  $2L$  and, therefore, the new frequency of the most unstable mode becomes equal to the quantity given by the  $f_a = u_c/(2L) = f_p/2$  relation [Danaila (1997)].

### 3.3.3 Streamwise evolution of the centerline jet mode

In this section, we are going to analyse the streamwise evolution of the most unstable mode at the jet center. To achieve this goal the energy spectra is treated as a function of the Strouhal number which is defined by the quantity  $fd_{jet}/\bar{u}_{jet}$ . Noting that the energy spectra of the axial velocity component  $u$  are examined at each measurement point of the jet flow. The measurement points cover all the ranges of the longitudinal coordinate from the vicinity of the jet (located at the  $x$ -coordinate equal to  $x/d_{jet} = 3.38$ ) until the zone further downstream of the potential core (located at the  $x$ -coordinate equal to  $x/d_{jet} = 34.03$ ) through the intermediate regions of the flow. The usefulness of this analysis is that it will allow us to follow the evolution of the different unstable modes that appear in the flow and to deduce the nature of the most unstable mode (absolute or convective), which is a fundamental information for both jet dynamics and jet control. In addition, the analysis is based on the average of six spectra obtained from portions of LDA signals com-

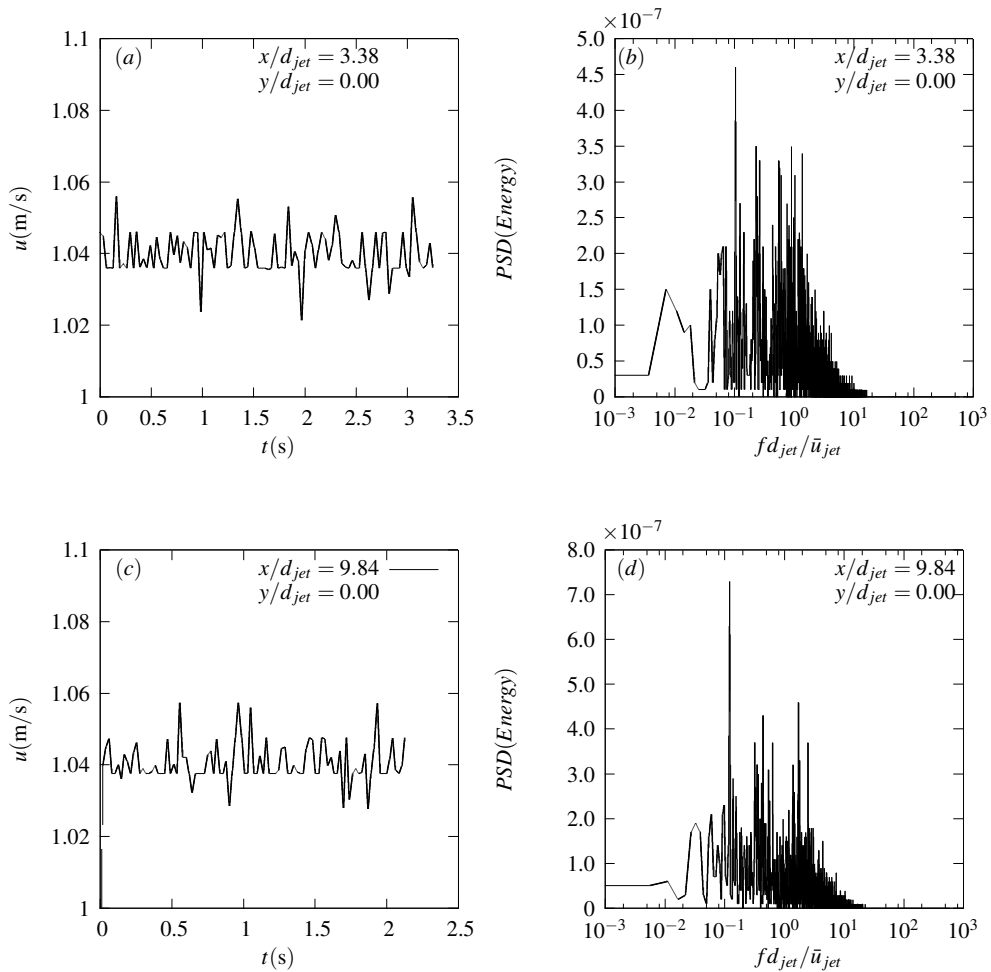


Figure 11: Temporal spectra of the streamwise velocity at the center region of the round air jet (emission velocity equal to  $\bar{u}_{jet} = 1.04m/s$  corresponds to a Reynolds number equal to  $Re = 832$ ). (a) Time series of the streamwise velocity  $u$  at several downstream positions. (b) Spectra of energy, obtained by the Fourier transform, at several downstream positions.

posed of  $2^{12}$  (or 4096) samples without overlap where the signals are acquired at a sampling rate of 100kHz corresponding to a signal duration equal to 40ms. We show in Fig. 11 and Fig. 13 the linear energy spectra data of the streamwise velocity component  $u$  for several longitudinal positions located by the coordinate  $x/d_{jet}$

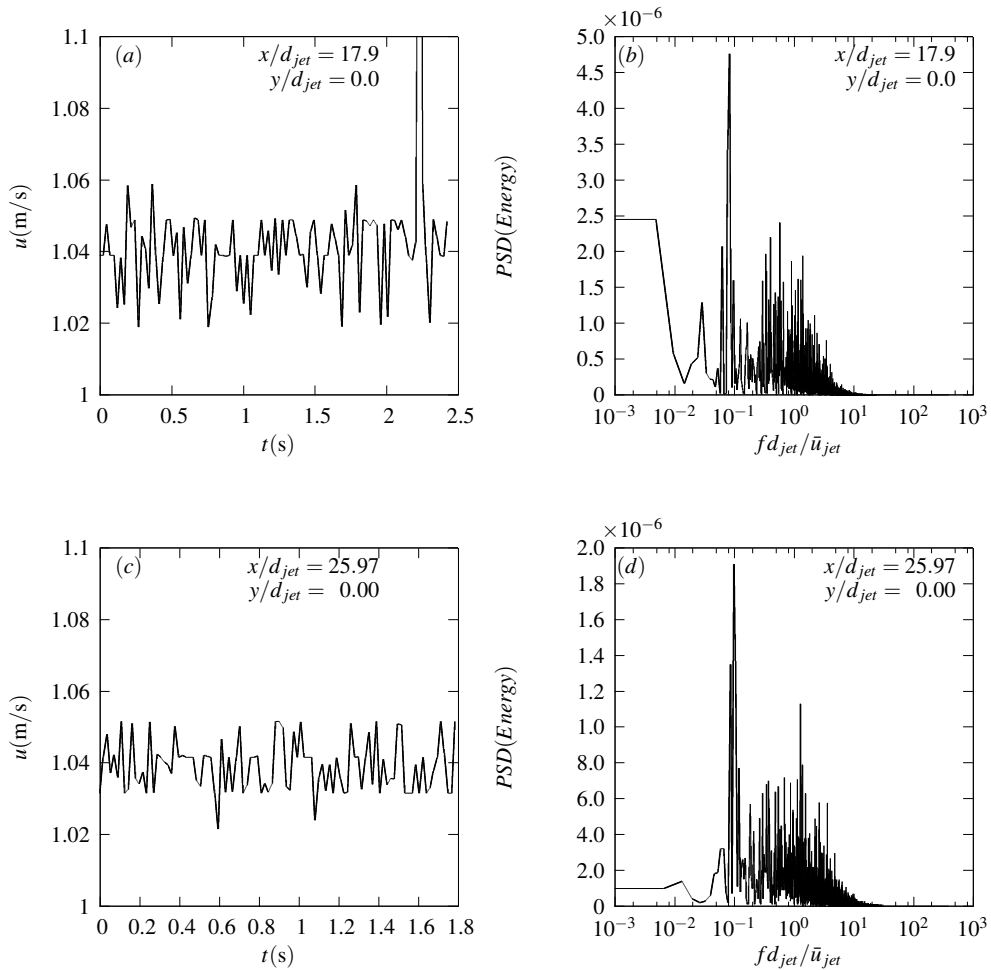


Figure 12: Temporal spectra of the streamwise velocity at the center region of the round air jet (emission velocity equal to  $\bar{u}_{jet} = 1.04m/s$  corresponds to a Reynolds number equal to  $Re = 832$ ). (a) Time series of the streamwise velocity  $u$  at several downstream positions. (b) Spectra of energy, obtained by the Fourier transform, at several downstream positions.

and at the centerline jet, namely at the transversal coordinate given by the quantity  $y/d_{jet} = 0.0$ . It is worth to note that the linear energy spectra provide details on the dominant frequencies which may exist in the investigated flow. We notice that for the first measurement point, as shown by Fig. 11b; which is obtained by

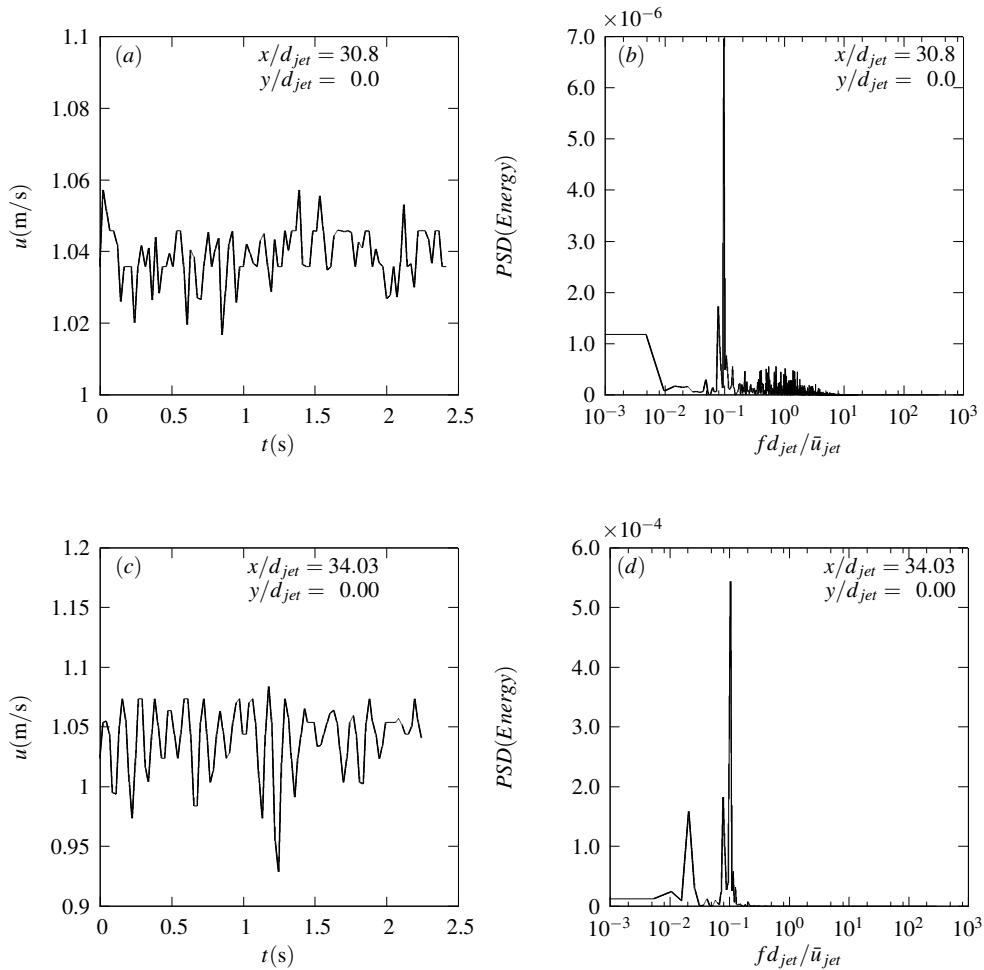


Figure 13: Temporal spectra of the streamwise velocity at the center region of the round air jet (emission velocity equal to  $\bar{u}_{jet} = 1.04m/s$  corresponds to a Reynolds number equal to  $Re = 832$ ). (a) Time series of the streamwise velocity  $u$  at several downstream positions. (b) Spectra of energy, obtained by the Fourier transform, at several downstream positions.

spectral analysis of the  $u$  velocity time series Fig. 11a and released in the internal mixing region of the jet; which is defined by the  $xy$ -coordinates equal to the value ( $x/d_{jet} = 3.38, y/d_{jet} = 0.0$ ), the existence of a dominant peak frequency that can be linked to large-scale structures passage. It is worth to note that, in addition to the

dominant frequency peak, the energy spectrum of  $u$  velocity contains other peaks as shown in Fig. 11b. In other words, the most energetic movement can be expected at the higher frequency peak corresponding to a Strouhal number equal to the value  $Str = fd_{jet}/\bar{u}_{jet} = 0.11$ . In Fig. 11d we represent the energy spectrum of the  $u$  velocity time series given by Fig. 11c. In this figure which is calculated at the measurement point defined by the  $xy$ -coördinate given by  $(x/d_{jet} = 9.84, y/d_{jet} = 0.0)$ , we also remark the existence of several dominant frequency peaks. However, from this spectrum two remarks can be made: firstly, the most energetic frequency described by the Strouhal number, remains to be roughly at around  $Str = fd_{jet}/\bar{u}_{jet} = 0.11$  and secondly, the motion at the other frequencies is less perceptible in the axial direction as is the previous spectrum given by Fig. 11b. Nevertheless we notice that, the motion at the most unstable frequency becomes obviously dominant in the jet flow direction. At the measurement point located at the  $xy$ -coördinate  $(x/d_{jet} = 17.9, y/d_{jet} = 0.0)$  the  $u$  velocity energy spectrum shows that the dominant peak remains the same with a remarkable decrease for the other peaks as demonstrate the Fig. 12b, we also remark that this behavior still valid for the measurement point represented by the Fig. 12c. Noting that at the other measurement points taken farther downstream until the position defined by  $(x/d_{jet} = 34.03, y/d_{jet} = 0.0)$ , the least energy frequencies attenuate and the dominant frequency keep almost the same value fixing the Strouhal number at the value of 0.11. In short, as we can see clearly according to Fig. 11 and Fig. 13, frequency peaks, other than the most unstable one, tend to converge towards the lower values as we move farther downstream in the jet flow. As a conclusion, we remark that the vortex structures dimension increases along the jet length under the action of the pairing process.

In summary, the jet flow transition towards the turbulent state takes place at a streamwise distance  $x/d_{jet}$  measured from the inlet nozzle. The value of this location can be estimated by studying the axial evolution of the Reynolds stress  $\langle u'^2 \rangle / \bar{u}_{jet}^2$  according to the  $x/d_{jet}$  coördinate as shown in figure Fig. 14b. Noting that until the longitudinal position defined by  $x/d_{jet} = 30$  the flow is laminar in the potential core region because no increase in the turbulent kinetic energy can be observed in the centerline jet. It is worth to note that, the first saturation of the Reynolds stress is reached at about the streamwise location equal to  $x/d_{jet} = 34$  which is accompanied by a rapid and sudden increase of the constraints that equal to the value of 0.35%. Noting that, this image corresponds to the typical transition scenario in round jets evolving at a low Reynolds number [Danaila (1997)]. It results from the previous analysis that, the nature of the most unstable mode is convective and occurs at a Strouhal number at around 0.11. It is significant to note that, this result compares well with that find using tomography laser, with the same

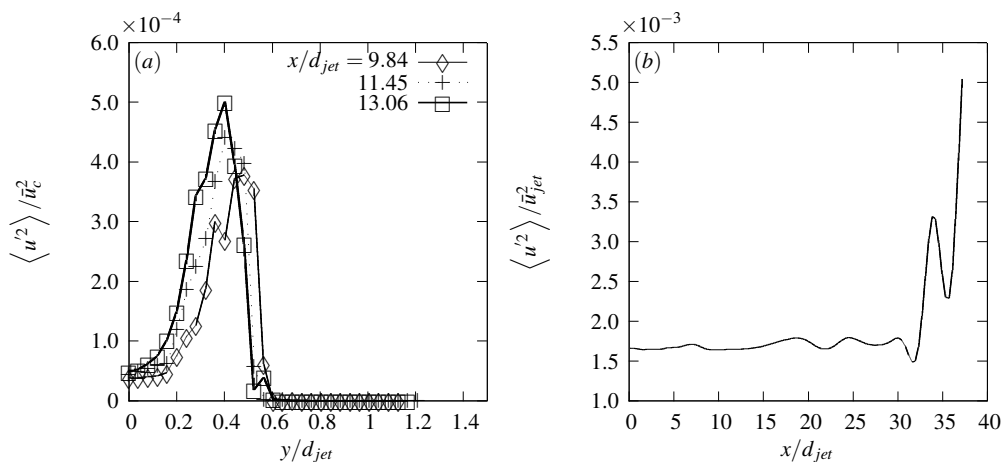


Figure 14: (a) Evolution of the Reynolds stress based on the streamwise velocity component  $u$  measured by LDA technique for different longitudinal locations  $x/d_{jet}$ . (b) Evolution of the turbulence intensity as function of the streamwise coordinate  $x/d_{jet}$ .

conditions used in the present work, which says that the most unstable mode occurs a Strouhal number equal to 0.102 ([Zaouali (2004)]) that makes an error between the two results of about 0.5%.

#### 4 Concluding remarks

The mode development of the coherent structures in the developing region, of an isothermal laminar round jet, is investigated by means of local measurement technique using Laser Doppler Anemometry LDA. It is significant to note that in the near-field of the round jet, flow spreading and momentum transfer are essentially dominated by the dynamics of the coherent structures which are occurring particularly by the existence of a velocity gradient in that region. In fact, the jet spreads and momentum transfer occur in a stepwise manner under the effect of the vortex interaction processes which include the mechanism of vortex formation and vortex merging. The vortex formation is determined from the point at which the transverse velocity fluctuations for the corresponding primary instabilities, namely the fundamental and its sub-harmonics, reach the saturation. Thus, to be able to follow the  $xy$ -evolution of the above process, LDA measurement covers the entire region from the jet center until the zone outside of the shear layer, in the transverse direc-

tion, and for stations farther downstream of the potential core, in the longitudinal direction. At the inlet jet, the profile of the streamwise mean velocity ( $\bar{u}/\bar{u}_{jet}$ ) is uniform and contains an inflexion point that is a necessary condition for transition occurring. However, the initial turbulence intensity is small so that the initial shear layer is considered laminar then the jet develops freely. The analysis of the jet mean fields shows the existence of the entrainment phenomenon and momentum transfer process. The measurement technique used in the present work has the advantage to prove the existence of several frequencies other than the frequency of the most unstable mode showing that the transition process is highly non-linear and occurs under the interaction between structures of various scales. The spectral analysis using the Fast Fourier Transform algorithm applied to the  $u(x, y, t)$  time series, show the existence of a dominant mode of a convective nature. The most unstable mode is characterized by a Strouhal number around to the value 0.11 that compares well with that found by using the tomography laser technique which is namely of about 0.102.

## References

- Abbassi, A.; Aissia, H. B.** (2014): Forced-mixed convection transition of a buoyant axisymmetric jet with variable properties. *Fluid Dynamics & Materials Processing*, vol. 10, no. 1, pp. 115–147.
- Abbassi, A.; Kechiche, N.; Aissia, H. B.** (2007): Prandtl-number effects on vertical buoyant jets in forced and mixed convection regimes. *Energy conversion & management*, vol. 48, pp. 1435–1449.
- Abid, M.; Brachet, M. E.** (1993): Numerical characterization of the dynamics of vortex filaments in round jets. *Phys. Fluids*, vol. 5, no. 11, pp. 2582–4.
- Batchelor, G. K.; Gill, A.** (1962): Analysis of the instability of axisymmetric jets. *J. of Fluid Mech.*, vol. 14, pp. 529–551.
- Ben Aissia, H.** (2002): *Étude numérique et expérimentale par imagerie et anémométrie laser Doppler d'un jet axisymétrique*. Thèse de doctorat, Univ. du centre, Tunisie, 2002.
- Crighton, D. G.** (1975): Basic principles of aerodynamic noise generation. *Prog. Aero. Sci.*, vol. 16, pp. 31–96.
- Crow, S. C.; Champagne, F. H.** (1971): Orderly structure in jet turbulence. *J. of Fluid Mech.*, vol. 48, pp. 547–591.
- Danaila, I.** (1997): *Étude des instabilités et des structures cohérentes dans la zone de proche sortie d'un jet axisymétrique*. Thèse de doctorat, Univ. de la Med. Aix-Marseille II, France, 1997.

- Drazin, P.; Reid, W.** (1981): *Hydrodynamic Stability*. Cambridge University Press.
- Grighton, D. G.; Gaster, M.** (1976): Stability of slowly diverging jet flow. *J. of Fluid Mech.*, vol. 77, pp. 397–413.
- Gutmark, E.; Ho, C.-M.** (1983): Preferred modes and the spreading rates of jets. *Physics of Fluids*, vol. 26, no. 10, pp. 2932–2938.
- Gutmark, E. J.; Grinstein, F. F.** (1999): Flow control with noncircular jets. *Annu. Rev. Fluid Mech.*, vol. 31, pp. 239–272.
- Ho, C. M.** (1981): Local and global dynamics of free shear layers. pp. 521–533.
- Ho, C. M.; Huang, L. S.** (1982): Subharmonics and vortex merging in mixing layers. *J. Fluid Mech.*, vol. 119, pp. 443–473.
- Hussain, F.; Zaman, K.** (1985): An Experiment study of organized motions in the turbulent plane mixing layer. *J. Fluid Mech.*, vol. 159, pp. 85–104.
- Kechiche, N.; Abbassi, A.; Filali, T.; Jay, J.; Aissia, H. B.** (2009): Spectral analysis of round jet instabilities at low Reynolds number. *Mécanique & Industries*, vol. 10, no. 4, pp. 447–454.
- Kibens, V.** (1980): Discrete noise spectrum generated by an acoustically excited jet. *AIAA J.*, vol. 18, pp. 434–441.
- Plaschko, P.** (1979): Helical instabilities of slowly divergent jets. *J. Fluid Mech.*, vol. 92, pp. 209–215.
- Rayleigh, L.** (1880): On the stability, or instability, of certain fluid motions. *Proc. London Math.Soc.*, vol. 11, no. 1, pp. 57–70.
- Reynal, L.; Harion, J. L.; Favre-Marinet, M.; Binder, G.** (1996): The oscillatory instability of plane variable density jets. *Physics of Fluids*, vol. 8, no. 4, pp. 993–1006.
- Winant, C. D.; Browand, F. K.** (1974): Vortex pairing: the mechanism of turbulent mixing-layer growth at moderate Reynolds numbers. *J. Fluid Mech.*, vol. 63, pp. 237–255.
- Yilmatz, T.; Kodal, A.** (2000): An analysis on coaxial jet flows using different decomposition techniques. *J. Fluid Structures*, vol. 14, pp. 359–373.
- Yu, M. H.; Monkewitz, P. A.** (1993): Oscillations in the near field of a heated twodimensional jet. *Journal of Fluid Mechanics*, vol. 255, pp. 323–347.
- Zaouali, Y.** (2004): *Étude tomographique des instabilités d'un jet axisymétrique à bas nombre de Reynolds par PIV et analyse des frontières*. Thèse de doctorat, Univ. du centre, Tunisie, 2004.

